

[<sup>14</sup>C]THF. This material was synthesized by the two methods shown in Schemes III and IV.

**Scheme III.** Labeled [2,3-<sup>14</sup>C]succinic acid (0.17 mg in 0.5 mL of 9:1 ethanol-water) was reduced with a slight excess of LiAlH<sub>4</sub> in THF. The resulting labeled 1,4-butanediol was diluted to the desired activity by adding unlabeled 1,4-butanediol and the mixture was added dropwise to hot diethyl phosphite.<sup>31</sup> The THF was distilled off as it formed. It was redistilled from LiAlH<sub>4</sub> to remove ethanol. Yields ranged between 60 and 70% and material having an activity of  $2.2 \times 10^5$  cpm/mL was obtained.

**Scheme IV.** A mixture of labeled [1,4-<sup>14</sup>C]succinic anhydride diluted to the desired activity with unlabeled succinic anhydride was refluxed with ethanol to form the half-ester. This ester was reduced with an excess of LiAlH<sub>4</sub> in ether using standard procedures. The labeled 1,4-butanediol was converted to THF as outlined in Scheme III.

[<sup>14</sup>C]Ethyl iodide. Material purchased from New England Nuclear was used without further purification.

**Chromatographic Separation of Coal Products.** The procedure developed by Burk and Sun was used.<sup>32</sup> Chromatography in 60–200 mesh, grade 62 MC/B silica gel was used. For a 6-g sample 1300 mL of hexanes, 2000 mL of benzene-hexanes (1:1 vol), and 1100 mL of THF were used followed by dissolving the column in concentrated aqueous NaOH and the liberated organics were dissolved in benzene. About 400 mL of solution was collected in fraction 2 as a transition between hexanes and the benzene-hexane fractions. Fraction 6 was material insoluble in THF and was not chromatographed.

**Liquid Scintillation Counting.** In LSC, the radiation emitted by the decaying nucleus interacts with dyes in the solution producing fluorescence which is detected by the instrument. In counting the coal-derived materials, several possible sources of error exist. If some of the coal-derived materials form colloidal species, the emitted particle may not escape from the colloid and

thus will not be counted. The colored materials formed from the coal may absorb some of the fluorescent radiation preventing its detection. Molecules derived from the coal may quench the fluorescence. Finally, materials derived from the coal may fluoresce themselves. The last three of these difficulties can be circumvented using an internal standard. Toluene labeled with <sup>14</sup>C was used as an internal standard in all of the solutions containing coal-derived materials and was used to determine the counting efficiency of these solutions. This would not correct for any errors introduced due to the presence of colloidal materials. Solutions were normally run at the highest dilutions possible compatible with good counting statistics. This minimizes the effects of the colored materials. Also, all solutions were allowed to stand for 24 h before counting to minimize problems with chemiluminescence. The LS 8100 instrument used permits the counting of fluorescence of specific energies and this was done. This also will minimize the effect of chemiluminescent materials.

Because of the possibility of the presence of colloidal materials, all samples were burned using the procedure of Davidson<sup>28</sup> and the CO<sub>2</sub> was absorbed by Oxysorb-CO<sub>2</sub> and counted using standard techniques. The agreement in most cases between the two methods is reasonable. With proper care, direct liquid scintillation studies of coal-derived materials can be done with reasonable accuracy. However the combustion technique is the more reliable.

**Acknowledgment.** We are grateful to the Fossil Fuel Division at the Department of Energy for support of this work. The comments and criticisms of Lee Stock were very helpful and are gratefully acknowledged. Without the excellent advice of Dr. Arthur Jungreis on LSC techniques we would still be doing experiments and we thank him for his generous contribution of time and counsel. The encouragement and experimental directions provided by Emmet Burk are acknowledged with thanks.

**Registry No.** [1-<sup>14</sup>C]Naphthalene, 16341-53-0; [2-<sup>14</sup>C]succinic anhydride, 70969-12-9; [2-<sup>14</sup>C]THF, 70969-13-0; [2-<sup>14</sup>C]succinic acid, 70969-14-1; [2-<sup>14</sup>C]-1,4-butanediol, 70969-15-2; ethyl iodide, 75-03-6.

(31) W. Vogt and S. Balasubramanian, *Angew. Chem., Int. Ed. Engl.*, **11**, 341 (1972).

(32) E. H. Burk, personal communication.

## Conformational Analysis of Pinanols<sup>†</sup>

John Texter and Eugene S. Stevens\*

*Department of Chemistry, State University of New York at Binghamton, Binghamton, New York 13901*

*Received February 5, 1979*

Empirical nonbonded atom interaction potentials are used in a Monte Carlo computational procedure to generate minimum conformational energy geometries for *trans*- and *cis*-2-pinanol, isopinocampheol, and neoisopinocampheol. The calculated dihedral angles of the cyclobutyl rings are in quantitative agreement with those determined by X-ray diffraction for a C<sub>3</sub>-substituted pinane. The preferred conformations of *trans*- and *cis*-2-pinanol, respectively, are chair and boat, and both of the pinocampheols studied also favor the boat conformation. These three boat conformations are not "full boats" and are more accurately described as skewed, semiboats.

Little is conclusively known about the preferred conformations of pinanols,<sup>1</sup> although these conformations govern the direction of certain reactions<sup>2-5</sup> and modulate the circular dichroism of the far-ultraviolet hydroxyl-centered  $\sigma^*/3s \leftarrow n$  transitions<sup>6</sup> reported by Kirk et al.<sup>7</sup> We propose to study (cf. Figure 1) the conformational stability of the methylnopinols I and II, isopinocampheol (III), and neoisopinocampheol (IV). The study of these species should lead to conclusions concerning the effects of configurational isomerizations of the C<sub>10</sub> methyl group about C<sub>2</sub> and of the hydroxyl group about C<sub>3</sub>.

Boat, chair, and nearly planar conformations for the six-membered ring have been observed in or predicted for a variety of ketone derivatives<sup>8</sup> of pinane, and a similar range of conformations has been assigned to the pinanols.

(1) D. V. Banthorpe and D. Whittaker, *Q. Rev., Chem. Soc.*, **20**, 373 (1966).

(2) A. K. Bose, *J. Org. Chem.*, **20**, 1003 (1955).

(3) W. D. Burrows and R. H. Eastman, *J. Am. Chem. Soc.*, **81**, 245 (1959).

(4) G. Zweifel and H. C. Brown, *J. Am. Chem. Soc.*, **86**, 393 (1964).

(5) F. J. Chloupek and G. Zweifel, *J. Org. Chem.*, **29**, 2092 (1964).

(6) J. Texter and E. S. Stevens, *J. Chem. Phys.*, **70**, 1140 (1979).

(7) D. N. Kirk, W. P. Mose, and P. M. Scopes, *J. Chem. Soc., Chem. Commun.*, **81** (1972).

(8) (a) For a recent compendium of references, see Table II in ref 8b; (b) J. Fournier, *J. Chem. Res. (S)*, 320 (1977).

<sup>†</sup>Supported in part by National Science Foundation Grant PCM77-21220.

Table I. Empirical Nonbonded Atom Interaction Potentials

atom pair	van der Waals, 6-9 <sup>a</sup>		Lennard-Jones, 6-12 <sup>b</sup>		Flory <sup>c</sup>		Kitaigorodsky <sup>d</sup>
	$\frac{A}{r^6} + \frac{B}{r^9}$		$-\frac{A}{r^6} + \frac{C}{r^{12}}$		$-\frac{D}{r^6} + Ee^{-4.6r}$		$3.5\left(\frac{-0.04}{z^6} + 8600e^{-1.3z}\right)$
	A/kcal mol <sup>-1</sup> Å <sup>6</sup>	B/kcal mol <sup>-1</sup> Å <sup>9</sup>	C/kcal mol <sup>-1</sup> Å <sup>12</sup>	D/kcal mol <sup>-1</sup> Å <sup>6</sup>	E/kcal mol <sup>-1</sup>	$z \equiv r/r_0$	$r_0/\text{Å}$
H...H	47	430	4 500	46.8	8 290	2.60	
H...C	128	2080	38 000	166.0	77 900	3.15	
H...O	124	1660	25 000	124.0	38 300	3.00	
C...C	370	9700	286 000	600.0	924 000	3.80	
C...O	367	8180	205 000	462.0	433 000	3.55	

<sup>a</sup> Reference 15. <sup>b</sup> Reference 16. <sup>c</sup> References 17 and 18. <sup>d</sup> References 18 and 19.

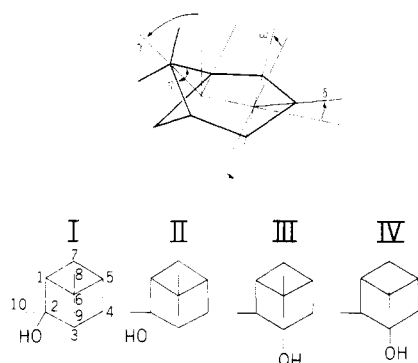


**Figure 1.** (Upper) Pinane carbon backbone illustrating the ring dihedral, twist, and puckering angles  $\delta$ ,  $\omega$ ,  $\eta$ , and  $\gamma$ . In our calculations the cyclobutyl ring parameters  $\eta$  and  $\gamma$  are used symmetrically. That is to say that  $\eta$  defines both the  $C_1-C_6-C_5$  and  $C_1-C_7-C_5$  angles, and  $\gamma$  defines precisely half of the supplement to the cyclobutyl ring puckering angle. (Lower) I, *trans*-2-pinanol (2 $\beta$ -hydroxy-10 $\alpha$ -pinane, *trans*-methylpinol, (1*R*,2*R*)-hydroxypinane); II, *cis*-2-pinanol (2 $\alpha$ -hydroxy-10 $\beta$ -pinane, *cis*-methylpinol, (1*R*,2*S*)-hydroxypinane); III, isopinocampheol (3 $\alpha$ -hydroxy-10 $\beta$ -pinane, (1*S*,3*S*)-hydroxypinane); IV, neoisopinocampheol (3 $\beta$ -hydroxy-10 $\beta$ -pinane, (1*S*,3*R*)-hydroxypinane).

However, details of the cyclobutyl ring structure (e.g., angles  $\eta$  and  $\gamma$ ) and six-ring deformations (e.g., the twist  $\omega$ ) have not been widely considered with respect to their ground state conformational stabilizing influences. In an early conformational study of pinanols,<sup>2</sup> puckering in the cyclobutyl ring was ignored, and this omission, in part, led to incorrect predictions of absolute configurations in several pinanols. X-ray diffraction studies of several substituted pinane-type systems<sup>9-11</sup> has since conclusively shown that the cyclobutyl ring adopts the normal puckered conformation characteristic of free, substituted cyclobutanes. The puckering angles  $\eta$  and  $\gamma$  are sensitive, however, to the particular type of  $C_2$ ,  $C_3$ , or  $C_4$  substitution. The strain energy of the cyclobutyl ring has been estimated to be on the order of half that of cyclobutane itself.<sup>12</sup> The cyclobutyl ring, however, has the effect of inducing strain energy in the six ring, so that analogies drawn with respect to the unstrained cyclohexane ring are no longer generally valid.<sup>13</sup> A particularly interesting aspect of this induced strain in the six ring is that the  $C_1-C_2-C_3-C_4-C_5$  array adopts somewhat the character of a cyclopentyl ring.<sup>1</sup> Finite  $\omega$  ( $\neq 0$ ) deformations are not usually considered as a sink for six-ring strain, although the  $C_1C_2C_4C_5$  array has been found to be nonplanar in an X-ray refinement<sup>9</sup> of

3-bromo-6,6-dimethylnorpinan-2-one and of the 3-chloro analogue.

In our investigation of the conformationally most favored angles  $\eta$ ,  $\gamma$ ,  $\delta$ , and  $\omega$  for the pinanols I-IV, we test an eclectic multidimensional energy minimization algorithm of simple design. Empirical nonbonded atom potentials have earned widespread acceptance,<sup>14</sup> and their use in the present investigation is appropriate because the conformational strain energy is induced by ring substituents. Adjoined to the empirical potential evaluation is a Monte Carlo sampling algorithm, which after convergence rests upon a mean field iterated to self-consistency along each coordinate (e.g.,  $\eta$ ,  $\gamma$ ,  $\delta$ , and  $\omega$ ). These computed results are finally compared with the available chemical, NMR, and X-ray evidence relating to the conformations of pinanols I-IV.

### Empirical Potential

The nonbonded atom interaction potential utilized in these calculations is, in fact, the arithmetic mean of four empirical potentials in popular use. These four component potentials are detailed in Table I<sup>15-19</sup> for the nonbonded atom interactions considered, and their combination was carried out in the following way. The *mean* potentials  $\bar{E}(x)$ ,  $x = \eta$ ,  $\gamma$ ,  $\delta$ , and  $\omega$ , were obtained by averaging the four potentials of Table I,  $E_a(x)$ ,  $E_b(x)$ ,  $E_c(x)$ , and  $E_d(x)$ , where the energy was expressed relative to the average absolute minimum. Each of the potentials  $E_a(x)$ , ...,  $E_d(x)$  was expressed relative to its own computed absolute minimum and was comprised at each  $x$  of the pairwise summation over all nonbonded atom pairs. Whenever one of the component potentials was evaluated over an interval  $x_i \leq x \leq x_f$  (e.g.,  $E_a(\omega)$  for  $-45^\circ \leq \omega \leq 45^\circ$ ), all of the other coordinates of variation (i.e.,  $\eta$ ,  $\gamma$ , and  $\delta$ ) were kept fixed. Standard bond lengths<sup>20</sup> were adopted for all calculations ( $d_{C-C} = 1.54$  Å,  $d_{C-H} = 1.09$  Å,  $d_{C-O} = 1.42$  Å,  $d_{O-H} = 0.98$  Å), the methyl group carbons were tetrahedrally coordinated, and the C-O-H angle was fixed at  $110^\circ$ . The methyl groups were fixed in staggered positions. The dihedral angles between the substituents attached to the  $C_1$ ,  $C_7$ ,  $C_2$ ,  $C_3$ , and  $C_4$  carbons were fixed at  $110^\circ$ , and these substituents were symmetrically arranged in a plane perpendicular to the plane of the closest three ring carbons. The  $C_1$  and  $C_5$  protons were oriented along a unit vector

(9) Y. Barrans, C. R. Hebd. Seances Acad. Sci., 259, 796 (1964).  
 (10) L. Kutschabsky, Z. Chem., 9, 31 (1969).  
 (11) G. Reck and L. Kutschabsky, Acta Crystallogr., Sect. B, 26, 578 (1970).  
 (12) D. V. Banthorpe and D. Whittaker, Chem. Rev., 66, 643 (1966).  
 (13) T. Hirata, Bull. Chem. Soc. Jpn., 45, 3458 (1972).

(14) A. I. Kitaigorodsky, Chem. Soc. Rev., 7, 133 (1978).  
 (15) D. A. Rees and P. J. C. Smith, J. Chem. Soc., Perkin Trans. 2, 830 (1975).  
 (16) R. A. Scott and H. A. Scheraga, J. Chem. Phys., 45, 2091 (1966).  
 (17) G. N. Ramachandran, C. M. Venkatachalom, and S. Krimm, Biophys. J., 6, 849 (1966).  
 (18) V. S. R. Rao, P. R. Sundararajan, C. Ramakrishnan, and G. N. Ramachandran in "Conformation of Biopolymers", Vol. 2, G. N. Ramachandran, Ed., Academic Press, New York, N.Y., 1967, pp 721-737.  
 (19) A. I. Kitaigorodsky, Tetrahedron, 14, 230 (1961).  
 (20) J. W. H. Kao and A. Chung-Phillips, J. Chem. Phys., 65, 2505 (1976).

formed by the sum of the direction cosines to the respective C<sub>1</sub> and C<sub>5</sub> substituents.

### Computational Procedure

The conformational energy minimization algorithm utilized here is a Monte Carlo mean-field approach, where the field is restricted to the nonbonded atom pairwise interaction limit. This restriction is not a necessary feature of our energy minimization algorithm; we utilize the empirical potentials described above because the evaluation of these potentials is extremely simple, straightforward, and rapid. Some essential advantages of our algorithm are that it is particularly applicable to multi-dimensional parameter (bond lengths, bond angles) searches in that computational time increases linearly with the degrees of freedom investigated, it is easily directed to convergence which results in a self-consistent mean field, and it is susceptible to the ordering of relative energy minima. Monte Carlo sampling is not new to the field of conformational energy analysis, and it is standard in many techniques used to evaluate theories of condensed media. The hybridization of Monte Carlo sampling and self-consistent mean-field interactions appears to be a useful contribution of the present study. The Monte Carlo nature of our algorithm refers to the random selection of various parameters over specified intervals with uniform probability density. These random selections are made with the aid of a random number "generator", which is a computer library function subroutine that provides, upon demand, numbers between 0 and 1 which are uniformly distributed over the unit interval. Our algorithm is described in terms of the following steps.

**Step 1.** An interval of variation,  $I^n(x)$ , is defined for each search coordinate  $x = \eta, \gamma, \delta$ , and  $\omega$ , where  $I^n(x) = [x_i, x_f]$  and  $n$  indexes the iteration. The  $I^0(x)$  we initially set rather arbitrarily, and the  $I^n(x)$ ,  $n \geq 1$ , are subsequently adjusted (as described in step 3) until the iterative convergence criteria (cf. step 3) are met. In our pinanol calculations, we utilized the following set of initial iteration intervals for I-IV:  $I^0(\eta) = [60^\circ, 90^\circ]$ ;  $I^0(\gamma) = [0^\circ, 45^\circ]$ ;  $I^0(\delta) = [-90^\circ, +90^\circ]$ ;  $I^0(\omega) = [-45^\circ, +45^\circ]$ . It will be subsequently seen that when convergence is reached we have  $I^n(x) \simeq I^{n-1}(x)$  for each coordinate  $x$ .

**Step 2.** This step is repeated in its entirety for each coordinate  $x$  and iteration  $n$ . We define the mean-field potential  $\langle E(x) \rangle^n$  as the arithmetic mean of  $j$  mean potentials,  $\hat{E}_k^n(x)$  ( $k = 1, \dots, j$ ), defined in the preceding section, and where the final values in  $\langle E(x) \rangle^n$  are expressed relative to the accompanying absolute minimum. Each of the mean potentials  $\hat{E}_k^n(x)$  is evaluated over the same interval  $I^n(x)$ . The Monte Carlo aspect comes into play here where for each  $k$ , the coordinates  $y \neq x$  are selected at random in the respective intervals  $I^n(y)$ . Thus the  $j$   $\hat{E}_k^n(x)$  represent mean potentials calculated with  $j$  distinct sets of fixed  $y$  coordinates,  $y \neq x$ , and hence  $\langle E(x) \rangle^n$  describes a potential obtained in a mean field. The calculations reported in the present study utilized a  $j$  of 50 (trials) for each iteration. The mean potentials  $\hat{E}_k^n(x)$  were evaluated at 8-20 equispaced points throughout the interval  $I^n(x)$ , so that the resulting mean field potentials  $\langle E(x) \rangle^n$  were evaluated at the same 8-20 points.

**Step 3.** In order to give convergence discriminating meaning, we invoke an energy criterion by which the  $I^{n+1}(x)$  are selected depending on the  $\langle E(x) \rangle^n$ . Let  $\epsilon$  denote this energy with the criterion that  $I^{n+1}(x) = [x_i, x_f]$  where  $\langle E(x) \rangle^n \leq \epsilon$  for  $x_i \leq x \leq x_f$ ,  $\langle E(\bar{x}) \rangle^n = 0$  for some  $\bar{x} \in I^{n+1}(x)$ , and  $\langle E(x) \rangle^n > \epsilon$  for  $x < x_i$  and  $x > x_f$ . In our calculations we arbitrarily chose  $\epsilon$  to be on the order of thermal energy, 0.6 kcal mol<sup>-1</sup>, and a smaller value could

Table II. Calculated Geometries for Pinanol Conformational Energy Minima<sup>a</sup>

pinanol	angles, deg				relative energy, kcal mol <sup>-1</sup>
	$\delta$	$\omega$	$\eta$	$\gamma$	
Ia	-52	2	84	25	7
Ib	35	1	84	23	22
II	36	10	83	24	0
III	33	11	84	23	22
IVa	25	11	85	24	49
IVb	-49	7	85	25	56

<sup>a</sup> The conformational angles  $\delta$ ,  $\omega$ ,  $\eta$ , and  $\gamma$  are defined in Figure 1.

probably not be justified. We do wish to stress the inherent uncertainties involved in these potential energy evaluations. Under the above criteria, we see that convergence can be defined as  $I^n(x) \rightarrow I^{n+1}(x)$  for each coordinate as  $n$  increases. We should also stress the interactive nature of our algorithm and further that we do not claim that an arbitrary choice of  $I^0(x)$  will necessarily automatically lead to convergence as defined above. The most common type of anomaly encountered is that at some iterative stage, say with the  $I^m(x)$ , one or more of the ensuing  $\langle E(x) \rangle^m$  may not have an interior minimum, so that the generation of the  $I^{m+1}(x)$  is blocked. A redefinition (e.g., an expansion) of  $I^m(x)$  usually suffices to remove the  $I^m(x) \rightarrow I^{m+1}(x)$  blockage. Another type of anomaly to be considered arises for certain  $x$  when a given  $I^m(x)$  is sufficiently large, where more than one relative minimum is observed in the resulting  $\langle E(x) \rangle^m$ . In this situation the problem is best treated by treating each of these relative minima separately (i.e.,  $\langle E(x) \rangle^m \rightarrow I_a^{m+1}(x)$  &  $I_b^{m+1}(x)$  where  $a$  and  $b$  respectively surround the two minima observed in  $\langle E(x) \rangle^m$ ). When convergence of the separate  $a$  and  $b$  tracks leads to distinct minimum energy geometries, a simple calculation can be carried out to order  $a$  and  $b$  with respect to each other.

**Step 4.** Steps 1-3 are repeated cyclicly until the convergence of step 3 is achieved. At this stage it is straightforward to check the self-consistency of the final iterates by defining  $I^\infty(x)$  as the respective minima points, fixing the respective  $x (=I^\infty(x))$ , and then evaluating  $\langle E(x) \rangle^\infty$  over  $I^0(x)$  where for all  $y \neq x$ ,  $y = I^\infty(y)$ . In the case that the minimum in  $\langle E(x) \rangle^\infty$  coincides with the point  $I^\infty(x)$ , self-consistency is proven. In cases where multiple relative minima exist along a single coordinate, the correct relative ordering is achieved straightforwardly by the evaluation of the  $\langle E(x) \rangle^\infty$ . When separate "a and b" tracks lead to final geometries which differ in more than one coordinate, relative ordering can be obtained by tabulating the total nonbonded interaction energy for each geometry.

### Results and Discussion

The results of our calculations are summarized in Table II. Each angle  $x$  is that which makes  $\langle E(x) \rangle = 0$  in the mean field of the other coordinates. The indicated relative energies were calculated with the respective fixed  $\delta$ ,  $\omega$ ,  $\eta$ , and  $\gamma$  angles. The self-consistency of these results was checked by the methods of step 4. Relative boat and chair minima were both found for alcohols I and IV.

Uniform results were obtained for the cyclobutyl ring dihedral angles  $\eta$  and  $\gamma$ . The calculated  $\gamma$  values ranging from 23 to 25° are in close agreement with the 24.3° obtained<sup>11</sup> for 3-[(*N*-methylamino)methyl]pinane hydrobromide by single-crystal X-ray diffraction. The range of 83-85° we determined for  $\eta$  is also in agreement with X-ray data,<sup>11</sup> where a value of 85° was found for the

$C_1-C_6-C_5$  angle and  $83^\circ$  was found for the  $C_1-C_7-C_5$  angle. This agreement between calculated and experimentally determined values of  $\eta$  and  $\gamma$  lends credence, we believe, to the validity of our calculated  $\delta$  and  $\omega$  values, where comparison with experiment is not so straightforward. While the cyclobutyl ring parameters exhibit an expected uniformity, variations in the  $C_{10}$  methyl and hydroxyl configurations induce an interesting boat-chair variability in the calculated relative strain energy (cf. Table II), which energy increases in the order  $II < Ia < Ib \sim III < IVa < IVb$ . Except for *trans*-2-pinanol (I), the lowest energy conformations are (semi) boat, and all of the energy minima geometries exhibit an  $\omega$  twist, to reduce the interactions between the *gem*-dimethyl bridge and the hydroxyl and  $C_{10}$  methyl groups.

The 2-pinanol isomers have not been as widely studied as have the isopinocampheols. Our calculations suggest that I and II favor the chair (Ia) and boat conformations, respectively, which is in agreement with the favored conformations cited for *trans*- and *cis*-pinane.<sup>1</sup> The  $C_{10}$  methyl group is fixed in a pseudo-equatorial position in both the chair (Ia) and boat (II) conformations, and both the hydroxyl groups are therefore directed axially. Our calculated boat conformation II differs from the chair conformation suggested earlier,<sup>3</sup> where the hydroxyl group was equatorially projected. However, the axial and sterically least hindered projection of the hydroxyl group in II is fully consistent with II exhibiting a greater acetylation reactivity than in I<sup>3</sup> where the axial hydroxyl is somewhat sequestered.

Our calculations predict that isopinocampheol (III) is more stable than neoisopinocampheol (IV) and that the  $C_{10}$  methyl groups in both III and IV adopt equatorial positions in the ground-state conformations. These predictions are in full agreement with the analysis of

Banthorpe and Whittaker,<sup>12</sup> which was based on varied esterification and deesterification rates. Zweifel and Brown<sup>4</sup> have predicted that the extreme boat and chair conformations for III and IV would not be favored, since the NMR data of Erskin and Knight<sup>21</sup> indicated that the  $C_{10}$  methyl protons in both compounds experience nearly identical chemical shifts and hence the relative positions of the  $C_{10}$  and  $C_9$  methyl groups must be very similar in III and IV. It was suggested<sup>4</sup> that a planar, "cyclopentyl" conformation for the  $C_1-C_2-C_3-C_4-C_5$  array could account for this invariance in the  $C_{10}$  methyl proton chemical shifts. As our calculations show (Table II), the semiboat conformation for III and IVa gives a reasonable account of the constancy in the  $C_{10}-C_9$  spatial arrangement. We found that the strictly planar conformations were highly sterically excluded relative to the semiboat minima with barriers on the order of 83 (III) and 64 kcal/mol (IVa).

In summary, it appears that the configuration at  $C_2$  of the  $C_{10}$  methyl group controls the conformation (semiboat or chair) of pinanols. The Monte Carlo empirical conformational energy algorithm we have here tested appears to give reliable results, at least for the cases studied here, in searching over multiple degrees of freedom. We reiterate that the sole use of primitive nonbonded atom interaction potentials is not a necessary feature of our algorithm. However, it has been demonstrated repeatedly<sup>14</sup> that such potentials often give results which are competitive with the most sophisticated computational schemes available.

**Registry No.** I, 35408-04-9; II, 35519-42-7; III, 24041-60-9; IV, 35998-01-7.

(21) R. L. Erskin and S. A. Knight, *Chem. Ind. (London)*, 1160 (1960).

## Conformational Analysis of N-Acyl Derivatives of 1-Aza-3-cyclohexanone<sup>†</sup>

Jerry A. Hirsch

Department of Chemistry, Seton Hall University, South Orange, New Jersey 07079

Received October 20, 1978

Ground-state rotamer energy differences and amide rotation barriers are evaluated for a series of N-acyl-3-piperidones by using carbon-13 NMR. The effects of substituents in the six-membered ring and of the acyl group on these properties are considered. For a given acyl group, amide rotation barriers are in the order 4-piperidone < morpholine < piperidine < 3-piperidone. Use of chemical-shift data to evaluate preferred rotamers is probed, exposing anomalous behavior on the part of the ring carbonyl group and important acyl group influences. An electrostatic interaction is required to explain some of the experimental results.

Amide rotation barriers have been extensively studied,<sup>1</sup> yet there have been few attempts to systematically evaluate the various steric and electronic influences on the barrier heights. Reisse and co-workers<sup>2</sup> and Yoder's group<sup>3</sup> have presented evidence that electron-donating substituents attached to the amide carbonyl (or thiocarbonyl<sup>2</sup>) groups result in electrostatic lowering of the barrier to rotation. Direct resonance interactions<sup>3</sup> also play a role. Steric factors are also evident,<sup>1,2</sup> with larger substituents producing lower barriers because of ground-state repulsive forces.

In our previous study,<sup>4</sup> we utilized variable-temperature carbon-13 magnetic resonance (<sup>13</sup>C DNMR) to investigate amide rotation barriers in a series of N-acylated six-membered nitrogen heterocycles (1-4), where steric factors

(1) W. E. Stewart and T. H. Siddall III, *Chem. Rev.*, **70**, 517 (1970); L. M. Jackman in "Dynamic Nuclear Magnetic Resonance Spectroscopy", L. M. Jackman and F. A. Cotton, Eds., Academic Press, New York, 1975, Chapter 7.

(2) C. Piccini-Leopardi, O. Fabre, D. Zimmerman, J. Reisse, F. Cornea, and C. Fulea, *Can. J. Chem.*, **55**, 2649 (1977).

(3) M. D. Wunderlich, L. K. Leung, J. A. Sandberg, K. D. Meyer, and C. H. Yoder, *J. Am. Chem. Soc.*, **100**, 1500 (1978).

(4) J. A. Hirsch, R. L. Augustine, G. Koletar, and H. G. Wolf, *J. Org. Chem.*, **40**, 3547 (1975).

<sup>†</sup> Dedicated to Professor Egbert Havinga of the University of Leiden on the occasion of his retirement.